Received: 18 May 2021 | Revised: 19 November 2021 | Accepted: 29 November 2021 | Published on: 14 December 2021

DOI: 10.1002/joc.7481

RESEARCH ARTICLE

International Journal of Climatology RMetS

Synoptic circulation changes over Central Europe from 1900 to 2100: Reanalyses and Coupled Model Intercomparison Project phase 6

Pedro Herrera-Lormendez[1] | **Nikolaos Mastrantonas**[1,2] | **Hervé Douville**[3] | **Andreas Hoy**[1] | **Jörg Matschullat**[1]

[1]Interdisciplinary Environmental Research Centre, TU Bergakademie Freiberg, Freiberg, Germany

[2]European Centre for Medium-Range Weather Forecast, Reading, UK

[3]Centre National de Recherches Météorologiques, Météo-France/CNRS, Toulouse, France

Correspondence
Pedro Herrera-Lormendez, Interdisciplinary Environmental Research Centre, TU Bergakademie Freiberg, Freiberg, Germany.
Email: pedro.herrera-lormendez@ioez.tu-freiberg.de

Funding information
H2020 Marie Skłodowska-Curie Actions, Grant/Award Number: 813844; EU International Training Network (ITN) Climate Advanced Forecasting of sub-seasonal Extremes (CAFE)

Abstract

While the evidence for anthropogenic climate change continues to strengthen, and concerns about severe weather events are increasing, global projections of regional climate change are still uncertain due to model-dependent changes in large-scale atmospheric circulation, including over North Atlantic and Europe. Here, the Jenkinson–Collison classification of daily circulation patterns is used to evaluate past and future changes in their seasonal frequencies over Central Europe for the 1900–2100 period. Three reanalyses and eight global climate models from the Coupled Model Intercomparison Project phase 6, were used based on daily mean sea-level pressure data. Best agreement in deriving relative frequencies of the synoptic types was found between the reanalyses. Global models can generally capture the interannual variability of circulation patterns and their climatological state, especially for the less frequent synoptic types. Based on historical data and the shared socioeconomic pathway 5 scenario, the evaluated trends show more robust signals during summer, given their lesser internal variability. Increasing frequencies were found for circulation types characterized by weak pressure gradients, mainly at the expense of decreasing frequencies of westerlies. Our findings indicate that given a high-emission scenario, these signals will likely emerge from past climate variability towards the mid-21st century for most altered circulation patterns.

KEYWORDS

anthropogenic climate change, circulation type classification, CMIP6, reanalyses, SSP5-8.5

1 | INTRODUCTION

Circulation classifications (CCs) simplify the infinite expressions of atmospheric circulation conditions into a concise number of recurrent atmospheric circulation patterns, typically associated with specific weather conditions over a particular region. CCs provide a valuable framework to assess past and future climate changes by isolating dynamical contributions (i.e., changes in circulation-type frequency or persistence) in multidecadal

variations of weather conditions. CCs can analyse the impact of both natural climate variability and external anthropogenic forcing at the regional scale. Beyond mirroring changes in mean climate, CCs also represent a powerful tool to investigate extreme events, which are often associated with specific atmospheric circulation patterns (Richardson *et al.*, 2020; Mastrantonas *et al.*, 2021).

Changes in frequency and severity of extreme events have long been recognized as one of the major threats posed by climate change (Seneviratne *et al.*, 2012). By definition, extreme events are rare; thus, it is often challenging to detect significant trends in available records. This is particularly true for precipitation extremes, given their limited spatio-temporal occurrence and the lack of spatial representativity of in situ measurements (Khairul *et al.*, 2018; Mastrantonas *et al.*, 2019). In contrast, daily circulation patterns can be reconstructed since the beginning of the 20th century or even earlier (Schwander *et al.*, 2017). They provide a valuable framework to analyse and interpret changes in long-term climate behaviour. While it is impossible even to attempt predicting distinct future weather in a literal sense when it comes to climatological time frames (many years to decades into the future), it appears feasible to elaborate future weather-type (WT) dynamics and their likely trigger-capacity for extremes on a wide range of time scales, from subseasonal to multidecadal. CCs group similar atmospheric patterns of mean sea level pressure (SLP), geopotential height and other atmospheric variables available in regular grids (Huth *et al.*, 2008). Obtained groups or classes are commonly known as circulation types (CTs) or weather types (WTs). Before the advent of computers, such "circulation catalogues" were subjectively categorized, based on synoptic experience and interpretation of the forecasters, and were mainly used in weather forecasting. Some of the best-known methodologies widely used for Europe are the (a) "Grosswetterlagen" catalogue, developed for Germany by Baur *et al.* (1944) and improved by Hess and Breszowsky (1952), (b) Lamb classification, created for the British Isles (Lamb, 1972), and (c) Schüepp's classification, focussing on Switzerland (Schüepp, 1979). However, new automated categorization became possible during the last few decades, given our ability to process increasingly larger data sets (Yarnal *et al.*, 2001).

One key reason to classify the different circulation conditions is their ability to realistically portray a strong association with other weather aspects (Jones *et al.*, 2014) and their usefulness to analyse atmospheric circulation variability with respect to frequency changes (Beck and Philipp, 2010). Some more recent applications have proven the usefulness of CCs in investigating relationships between large-scale atmospheric synoptic configurations and climate variables such as temperature or precipitation (Jacobeit *et al.*, 2003; 2017; Beck *et al.*, 2007; Hoy *et al.*, 2013a; 2013b; Hoy *et al.*, 2014; Vallorani *et al.*, 2018), and to evaluate CT trends during the 20th and early 21st century (Cahynová and Huth, 2016; Kučerová *et al.*, 2017; Stryhal and Huth, 2019b). The underlying general assumption is that human-induced changes in atmospheric circulation manifest themselves primarily in the frequency and persistence of recurrent CTs rather than in the spatial circulation patterns themselves. Such a statement can be tested a posteriori when using "dynamical" classification techniques without prior assumptions on CTs' number and specific definition.

Here, we investigate past and future frequency changes of synoptic circulation patterns based on an automatized version of Lamb's classification adapted by Jenkinson and Collison (1977) and commonly known as the Jenkinson–Collison automated classification (JC). This approach has become one of the most-used ones, given its simplicity to be adapted to other mid-latitude regions and its relatively easy interpretation of resultant CTs based on large-scale geostrophic flow (Jones *et al.*, 1993). This classification experienced a renaissance over the last two decades owing to the development of consistent spatiotemporal gridded datasets like reanalyses. Applications evaluating the ability of the classification to recreate the circulations patterns and their relationship with other atmospheric variables emerged from various mid-latitude regions: Scandinavia (Linderson, 2001), Iberia (Goodess and Jones, 2002; Lorenzo *et al.*, 2011), Taiwan (Lai, 2010), Chile (Sarricolea Espinoza *et al.*, 2014), Falkland Islands (Jones *et al.*, 2016), southwest Russia (Spellman, 2017), to evaluate their representation on climate model simulations (El Kenawy *et al.*, 2014; Otero *et al.*, 2018; Fernandez-Granja *et al.*, 2021) and to reconstruct European circulation conditions back to the 19th century, using reanalyses (Jones *et al.*, 2013), and the 18th century, based on observations (Delaygue *et al.*, 2019).

Global warming is expected to change the frequency of the circulation patterns as we start facing the dynamical response to increasing CO_2 levels and related changes in global surface temperature. Such circulation changes can either mitigate or enhance the changes in the behaviour of surface atmospheric variables (Belleflamme *et al.*, 2015; Räisänen, 2019) and which can result in direct impacts on extreme events like droughts, heatwaves, and heavy rains (Meehl and Tebaldi, 2004) given the strong influence of atmospheric circulation on climate at the regional scale (Shepherd, 2014). Several climate projections demonstrated, for example, (a) that

blocking situations might decrease in frequency and shift towards eastern Europe (Woollings *et al*., 2012; de Vries *et al*., 2013), though observed trends are sensitive to the choice of the blocking index and to large internal variability that complicates the detection of forced trends (Barnes *et al*., 2014; Cattiaux *et al*., 2016; Woollings *et al*., 2018), (b) higher probability of heat waves with longer mean duration, extent and intensity (Russo *et al*., 2015; Schoetter *et al*., 2015), as well as (c) an increase in the persistence of mild westerlies, which might contribute to warmer winter temperatures across much of the continent (Hoy *et al*., 2013b; Kučerová *et al*., 2017). Hence, it is crucial to understand if these variations can be explained by CT-frequency changes or simply by within-types' variations (Beck *et al*., 2007).

Therefore, this work focuses on evaluating CT-frequency changes, using some of the latest reanalyses and two experiments from the Coupled Model Intercomparison Project phase 6 (CMIP6). We aim at (a) comparing the ability of reanalyses and of global models to reproduce the winter and summer frequencies of the main synoptic patterns, and (b) detecting changes in these CTs' occurrences since the 1900s and to figure out whether evaluating a high emission scenario will drive significant changes in atmospheric circulation types.

Section 2 describes the different reanalyses and CMIP6 models we used. Section 3 explains the geographical space, the procedure involved in implementing the JC classification, the evaluation of the model's ability to reproduce the frequencies of the circulations and the methodology for evaluating past and future trends. Section 4 discusses the results. Conclusions are drawn in section 5.

2 | DATA

2.1 | Reanalyses

Reanalyses became one of the most-used datasets in studying weather and climate dynamics over past decades. They provide comprehensive and physically consistent reconstructions of past atmospheric conditions at the Earth's surface and across the different atmospheric levels by assimilating satellite and/or conventional observations in numerical weather models (Parker, 2016). We use $1° \times 1°$ latitude/longitude gridded daily SLP data from three state-of-the-art reanalyses and daily mean 2 m temperature (T2M) from only one dataset (ERA5) to investigate the relationship of these atmospheric types with European temperatures. The ERA5 reanalysis, distributed by the Copernicus Climate Change Service of the ECMWF, is the newest set of atmospheric reanalyses, embodying a detailed record of the global atmosphere. Data is currently available from 1950 to the present (Hersbach *et al*., 2020). The ERA-20C reanalysis by ECMWF is a 20th-century dataset. It covers 1900–2010 and assimilates surface pressure and marine wind observations only (Poli *et al*., 2016). The NOAA-CIRES 20th Century Reanalysis V3 (NOAA-20CRv3), created by the National Oceanic and Atmospheric Administration, assimilates a large set of surface pressure observations available for the 1836–2015 period (Slivinski *et al*., 2019). The assimilation of these observations allows for outputs that provide a realistic picture of synoptic situations over sufficiently well-observed regions like Europe. Here we use the 1900–2010 period from these last two reanalyses to compare their time span directly with each other.

2.2 | CMIP6 global climate models

The Coupled Model Intercomparison Project (CMIP) is an international collaborative framework designed to improve climate change knowledge. Recently, its sixth phase has seen the participation of an increasing number of global modelling centres and the coordination of a large variety of experiments (Eyring *et al*., 2016). These include, among other experiments, standard historical simulations, driven by observed radiative forcings, and new Shared Socioeconomic Pathways (SSP) scenarios, exploring a range of plausible future climates on how the world might evolve given the absence—or achievement—in the reduction of emissions and climate policy.

Here, daily mean SLP datasets from eight CMIP6 Global Climate Models (GCMs; hereafter also referred to as models) are employed to assess past and future large-scale circulation changes since the 20th century. Using different models allows capturing the high degree of variability in the circulations and their uncertainties by using four to six members in each GCM (Table 1). We employ the historical experiment using the data for the 1900–2010 and the Shared Socioeconomic Pathway 5 (SSP5-8.5) scenario covering the 2015–2100 time span. The historical simulation is based on the climate response, considering historically evolving forcings (e.g., emissions of short-lived and long-lived greenhouse gases [GHGs] and their concentrations, global gridded land-use forcings, solar forcing, stratospheric aerosol from volcanoes, etc.). As far as possible, it is based on observations (Eyring *et al*., 2016). SPP5-8.5 is used to assess future circulation changes; envisioning rapid economic growth driven by an energy-intensive, fossil fuel-based economy. This will result in the highest overall emissions compared to any other SSP, with resulting warming of 4.7–5.1°C by the end of the century (O'Neill *et al*., 2015; Riahi *et al*., 2017). This pathway was selected to effectively

TABLE 1 CMIP6 models used in the current study: Model names, corresponding institution, original resolution and number of realizations employed in the historical and SSP5 experiments

GCM name	Institution	Original lon–lat	Realizations
CNRM-CM6-1 (Voldoire, 2018)	Centre National de Recherches Météorologiques, France	1.4 × 1.4°	6
MPI-ESM1.2-LR (Wieners *et al.*, 2019)	Max Planck Institute for Meteorology, Germany	1.9 × 1.9°	6
IPSL-CM6A-LR (Boucher *et al.*, 2018)	Institute Pierre Simon Laplace, France	2.5 × 1.25°	6
MIROC6 (Tatebe and Watanabe, 2018)	Japan Agency for Marine-Earth Science and Technology, Japan	1.4 × 1.4°	6
EC-Earth3 (EC-Earth, 2019)	EC-Earth Consortium	0.7 × 0.7°	4
ACCESS-ESM1-5 (Ziehn *et al.*, 2019)	Commonwealth Scientific and Industrial Organisation, Australia	1.8 × 1.2°	6
HadGEM-GC31-LL (Ridley *et al.*, 2018)	Met Office Hadley Centre, UK	1.8 × 1.25°	4
UKESM1.0-LL (Tang *et al.*, 2019)	Met Office Hadley Centre, UK	1.8 × 1.25°	4

capture future changes in circulation frequencies if world development continues to strongly depend on fossil fuels. Similar to the former CMIP5 RCP8.5 scenario, SSP5-8.5 may appear excessively pessimistic for the late 21st century. Yet, it remains the best match out to mid-century under existing and foreseeable emission policies. Thus, it is a valuable framework to quantify physical climate risks, especially across the first half of the century (Schwalm *et al.*, 2020).

All GCM data underwent bilinear interpolation to a regular grid of 1° latitude by 1° longitude, consistent with the reanalyses' resolution.

3 | METHODS

The JC classification uses 16 gridded SLP points to classify daily circulation patterns, based on the calculation of the different flow features: That includes zonal and meridional flow components, resultant flow, zonal and meridional shear vorticity components, as well as total shear vorticity (detailed explanation about the corresponding equations in Jones *et al.*, 2013). This methodology can be adapted to practically any region in the midlatitudes, given its strong dependency on horizontal pressure gradients to derive any of the terms. Adaptation is possible by shifting the 16 grid points over the domain of interest and adjusting its latitude-dependent equations to represent the new central area. Here, we use the region delimited within 40°–60°N and 5°W–25°E centred over Germany (Figure 1). This area comprises most of central and a small part of western Europe as well as portions of the North and Mediterranean Seas. This selection allows capturing the wide range of synoptic circulations that transit from all directions and directly affect the predominant regional weather on a day-to-day basis.

Twenty-seven different CTs are obtained on a daily basis once the automated classification is performed. The original CTs are classified as follows: Low Flow (LF), characterized by weak pressure gradients, Anticyclonic (A) and Cyclonic (C), delimited as high- and low-pressure systems centred over the area. Hybrid CTs respond to slight variations in the A and C types' central positions and describe the direction of the main flow over the central area. Therefore, type AN corresponds to an Anticyclone with its centre shifted towards the west, creating a predominant Northerly flow over the region. This same naming convention follows the rest of the 16 hybrid types. Finally, the pure directional types correspond to those constellations when classification cannot be assigned directly to one of the main A or C circulations. Thus, isobars and the main flow cannot be considered dominated by a high or a low-pressure system, resulting in eight CTs named according to the corresponding dominant flow direction.

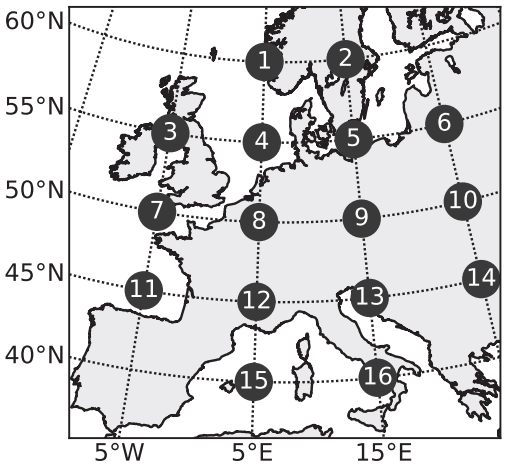

FIGURE 1 The 16-grid points used for the JC classification in this paper, centred over Germany

We reduced their number to 11, given the uneven occurrence distribution of CTs, especially when related to extreme weather events. The reduction in the number of synoptic types has long been suggested in previous studies, with seven types for the British Isles (Lamb, 1972) and eight types (Jones *et al*., 1993), where a hybrid type is given the same weight towards its major type. Here, we follow Delaygue's proposed simplification, favouring the A and C circulations (Delaygue *et al*., 2019) and combining the hybrid types by attributing them to their "pure" synoptic type (e.g., AN, ANE, AE, etc. becoming A, and CN, CNE, CE, etc. becoming C). However, unlike the UK's application, we retain all pure directional types as well as the Low Flow type and end up with a reduced number of 11 CTs (Table 2). This methodology is preferred as the reduced number of CTs bring important information about the directional nonmerged types and their connections with localized surface temperature conditions due to the vital role of large scale advection driven by pressure.

TABLE 2 Description and acronyms of the original 27 WTs, obtained from the classification, and resulting merged 11 types

CT categories	27 original weather types	11 merged weather types
Low flow	LF	LF
Anticyclone	A	A
Hybrid anticyclones	AN	
	ANE	
	AE	
	ASE	
	AS	
	ASW	
	AW	
	ANW	
Cyclone	C	C
Hybrid cyclones	CN	
	CNE	
	CE	
	CSE	
	CS	
	CSW	
	CW	
	CNW	
Pure directional	N	NW
	NE	N
	E	E
	SE	SE
	S	S
	SW	SW
	W	W
	NW	NW

Day-to-day synoptic types were obtained based on daily mean SLP pressure fields. In the ERA5 dataset, daily averages were built from 6-hourly data (0, 6, 12, and 18Z), whereas data from the remaining sources were directly available as daily averages. Subsequently, CTs are compared as seasonal relative frequencies for winter (DJF) and summer (JJA) seasons. Composites based on the ERA5 reanalysis were created based on the 1981–2010 period. We calculated daily SLP and T2M anomalies, where a 5-day moving average was used to compute a smooth daily mean climatology to obtain the corresponding temperature anomalies. A two-tailed Student's test computed significant T2M anomalies different from zero above the 95% confidence interval.

Subsequently, we employ two objective indices to measure the ability of the reanalysis and the GCMs to capture the characteristics of the CTs during the reference period of 1981–2010, as described by Perez *et al*. (2014). The scatter index (SI), defined as the root mean square error normalized by the mean frequency, compares the seasonal relative frequencies derived from the ERA-20C, NOAA-20CRv3 reanalyses and the eight global models with the resulting from ERA5. The SI is defined as follows:

$$\mathrm{SI} = \sqrt{\frac{\sum_{i=1}^{N}(p_i - p_i')^2}{N}} \Big/ \frac{\sum_{i=1}^{N}(p_i)}{N}, \tag{1}$$

where p_i denotes the winter or summer relative frequency of the ith CT from ERA5, p_i' the season's relative frequency derived from the remaining reanalyses and GCMs, and N represents the number of used circulation types (11 in our case). We evaluate the index across all members of each model, which allows us to illustrate their uncertainty. This index provides a measure of the skill of the reanalyses and the models to represent the climate status of the CTs. The scatter index of the standard deviations (stdSI) is employed to analyse the skill of the different datasets to represent the interannual climate variability throughout the reference period. Defined as

$$\mathrm{stdSI} = \sqrt{\frac{\sum_{i=1}^{N}(\mathrm{std}(p_i) - \mathrm{std}(p_i'))^2}{N}} \Big/ \frac{\sum_{i=1}^{N}(\mathrm{std}(p_i))}{N}. \tag{2}$$

It uses the annual values of relative frequencies of each CT during the 30 years of the reference period. The

lower the SI and stdSI, the better the performance of the GCM. Values larger than 1 would indicate a GCM with a lower simulation performance than the frequency of the synoptic situations obtained in the ERA5 reanalysis.

Subsequently, trends were analysed as resulting relative trend magnitudes based on the Theil–Sen estimator (Harrigan *et al*., 2018; Hannaford *et al*., 2021). Based on the 90th, 95th and 99th percentile statistical significance, they display only significant trends resulting from the nonparametric Mann–Kendall trend test. Calculations were conducted with the Python package pymannkendall (Hussain and Mahmud, 2019). The trend analysis was divided into two periods (past and future), with the past representing 1900–2010, computed from the ERA20C and NOAA-20CRv3 data, and compared against the ensemble mean winter and summer frequencies (CTs calculated along with each member and then averaged) of the CMIP6 historical simulation; while the future is based on the SSP8.5 scenario, covering the 2015–2100 period. ERA5 reanalysis is not included in the trend analysis due to the shorter period for which they are available. However, ERA5 data is used to study the spatial representation of the CTs and their present-day climate relationship with surface temperatures.

The Time of Emergence (TOE) is introduced to evaluate the point in time when long-term changes in the occurrence of circulation patterns emerge from the early 20th-century historical variability. We employ a modified version of the Signal Threshold method (Maraun, 2013) by outlining an upper and lower threshold demarcated by the CTs mean seasonal relative frequencies, resulting from all members used in each GCM. Such thresholds are defined by the corresponding 90th and 10th percentile, based on the 1900–1950 period. Later, a third-degree polynomial fit is adjusted to the mean seasonal frequency of each of the CTs and models. The year of emergence is expressed as the first year when the fitted line crosses the upper or lower limit (Figure 2). We avoid using the data before the 1900s to define these thresholds as we observed distinct inconsistencies in some of the resulting circulation frequencies. This behaviour was observed mainly in the Low Flow type. A substantial decrease in its occurrence appears in the NOAA-20CRv3 reanalysis and some models from the 1850s towards the end of the 19th century.

4 | RESULTS

4.1 | Spatiotemporal circulation-type characteristics

We use the ERA5 reanalysis, based on the 1981–2010 climatological period to show the composites of SLP and T2M daily anomalies for five of the main CTs. These synoptic circulations (Figures 3 and 4) are based solely on this source as they represent our closest approximation to reality. They demonstrate JC's ability to correctly capture the different CTs based on pressure fields and flow directions over the target region. The main differences in the seasonality of the different types materialize in the pressure gradients. We observe more intense (weaker) meridional gradients during winter (summer) as expected due to related meridional temperature gradients along the midlatitudes (Figure 3).

The corresponding Low Flow CT during winter is characterized by a very weak pressure gradient that complicates assigning a defined type of circulation.

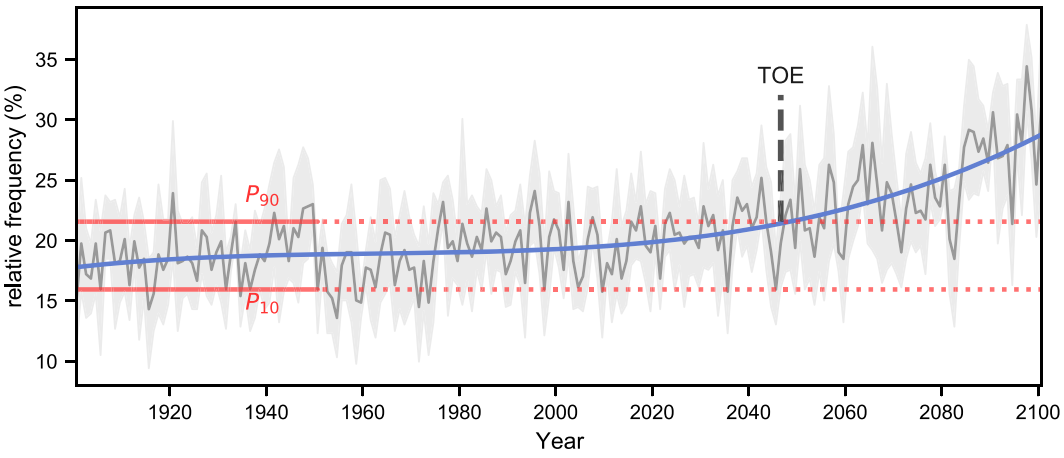

FIGURE 2 Calculation example of the time of emergence (TOE), based on the JJA relative frequency of the LF CT from the CNRM model. Upper and lower thresholds represent the 90th and 10th percentiles from 1900–1950 (continuous red line), considering the mean seasonal frequency among members. The solid blue line represents the third degree fitted polynomial for 1900–2100. TOE in each model is the year when the signal crosses the upper or lower threshold [Colour figure can be viewed at wileyonlinelibrary.com]

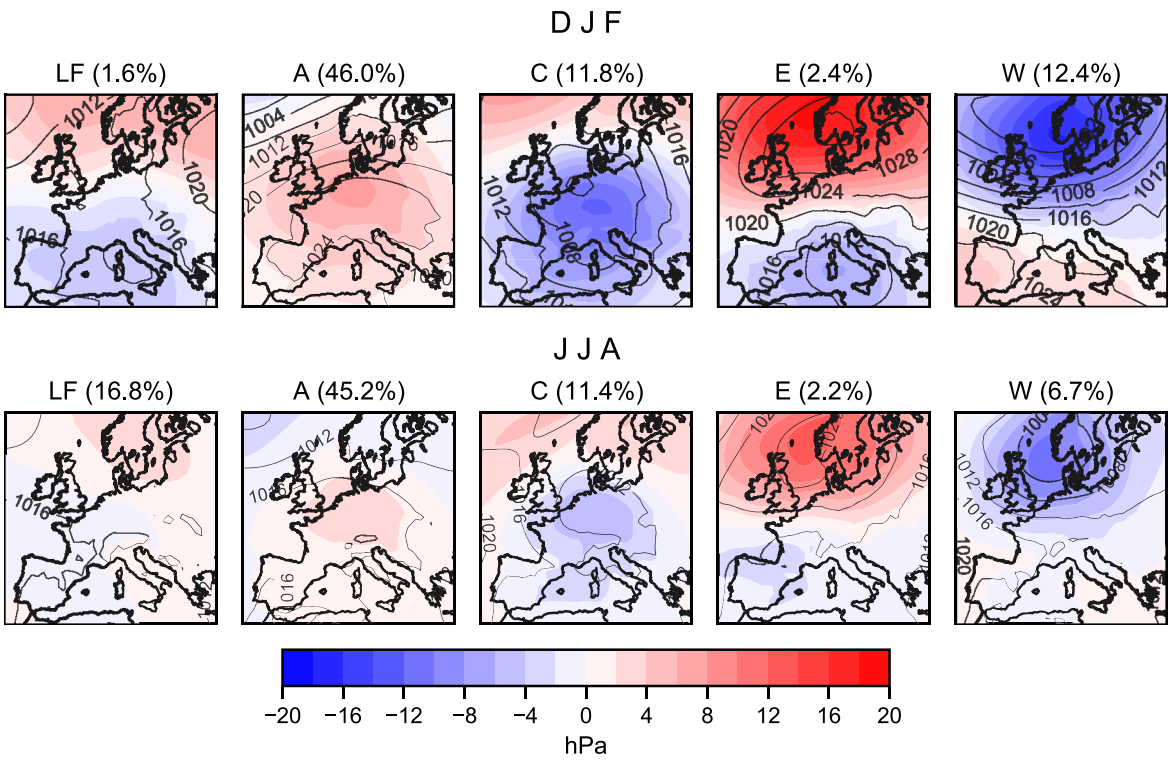

FIGURE 3 1981–2010 winter (DJF) and summer (JJA) SLP composites of mean (contour lines) and anomalies (shaded) of five CTs, based on the adapted JC classification for Europe. Percentages indicate their mean seasonal relative frequency based on the ERA5 reanalysis [Colour figure can be viewed at wileyonlinelibrary.com]

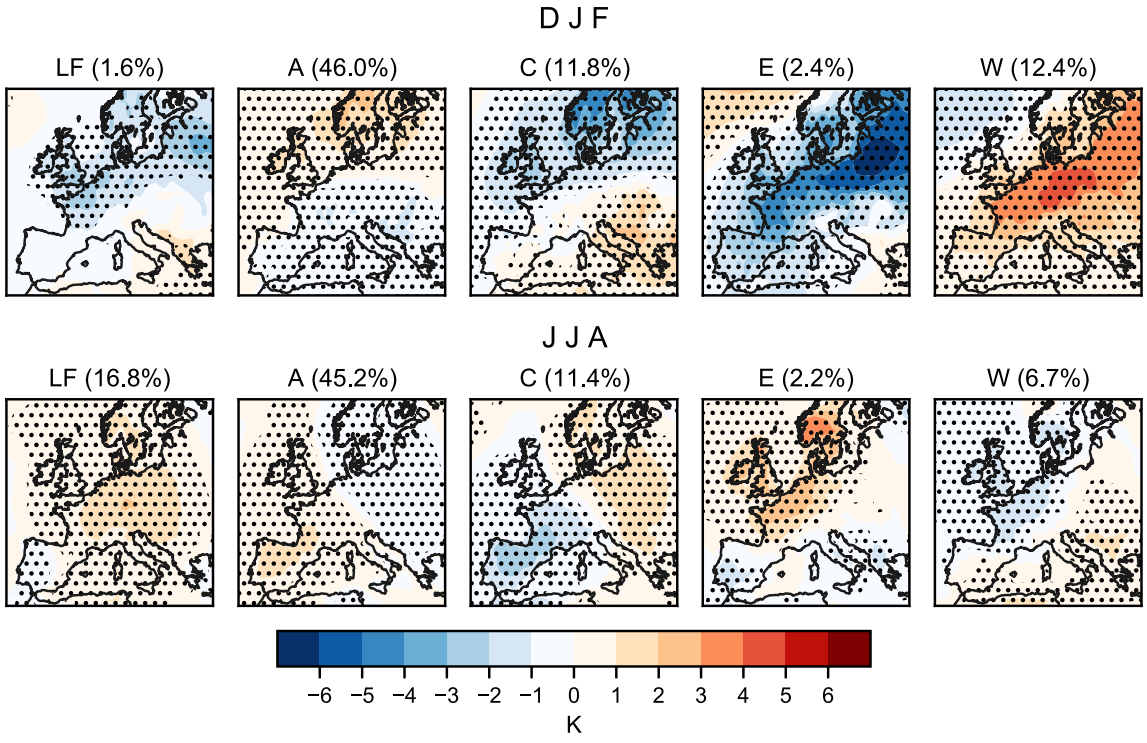

FIGURE 4 1981–2010 winter (DJF) and summer (JJA) composites of daily temperature anomalies (in K), related to five CTs. Dots show the significant anomalies (95% confidence), based on a two-tailed Student's test. Percentages indicate each circulation's mean seasonal relative frequency based on the ERA5 reanalysis [Colour figure can be viewed at wileyonlinelibrary.com]

LF-governed days are dominated by weak airflow and lack a defined direction of large-scale advection. They are linked to slightly colder temperatures over northern Europe, where anomalous positive SLP values appear to be related to high-pressure ridges during these events. On the contrary, summer is dominated by positive temperature anomalies, likely related to stationary air masses that heat up faster over continental areas influencing the daily temperatures (Figure 4). The merged A and C types, respectively, represent the two most frequent CTs occurring during the year, accounting for roughly 56% of total annual variability. Their effects on temperatures are well-defined, depending on flow direction. During summer, both circulation patterns depict a west–east divide, given their influence on temperatures. This effect is more evident in the cyclonic type, where we observe the southerly warm and the northerly cold sector towards the east and west of the domain, respectively. In contrast, the inverted sectors are observed in the anticyclonic circulation. However, it should be stated that even if the composites depict the centre of these synoptic patterns over Germany, by merging all hybrid types, we fail to capture information related to the small spatial variations in their central position over the domain. The remaining eight CTs are defined subject to their dominant flow direction; the eight cardinal directions represent them. Here, we show the easterly and westerly types as they are usually related to characteristic contrasting weather conditions. Easterlies, for example, are responsible for the advection of very cold temperatures from continental Eurasia during DJF. In contrast, westerlies favour milder temperatures, given their maritime origin during this season. Nevertheless, this effect is at the inverse during the JJA season. The easterly CT advects warmer and drier continental air resulting in positive temperature anomalies over the W-NW Europe. On the other side, the influence of wet milder westerlies results in slightly colder temperatures than usual over this area. The influence of the remaining synoptic patterns (Figures S1 and S2) confirms their strong correlation, depending on the large-scale patterns' dominant wind direction. Southerlies and dominant Westerly types are commonly associated with positive temperature anomalies, whereas the contrary is observed for Easterly and Northerly circulation patterns. These composites demonstrate that the classification in the ERA5 reanalyses well captures CTs and their effects on European temperature fields. However, the limitations arising when using only a single dataset to evaluate these links have to be considered as the results might differ from one reanalysis to another, as previously pointed out by Stryhal and Huth (2017).

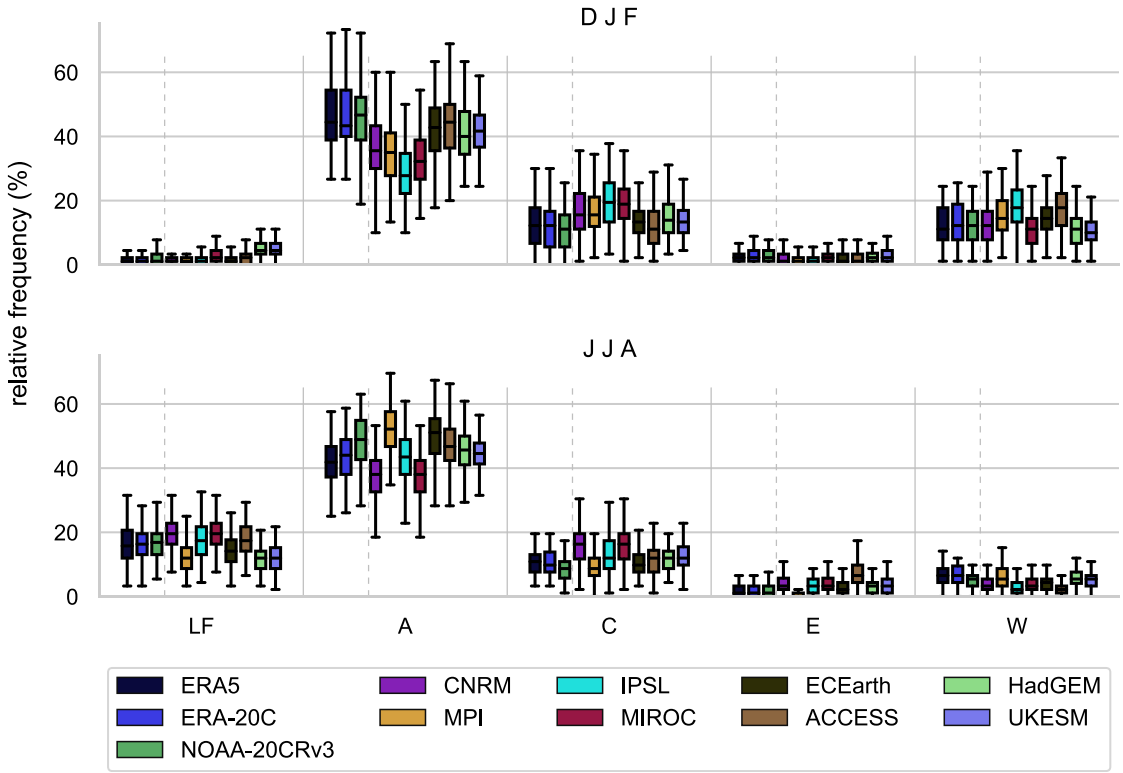

FIGURE 5 DJF and JJA relative frequencies of five simulated CTs. Comparison with the 1981–2010 period and the different data sources [Colour figure can be viewed at wileyonlinelibrary.com]

Derived seasonal relative frequencies can be seen in Figure 5, after computation based on daily SLP data from reanalyses and CMIP6 GCMs. The boxplots show the same five CTs as discussed before when considering the 1981–2010 period. The best agreement results when computing the CTs based on the reanalyses datasets. The main differences appear when obtaining the circulation patterns with some of the global models. Anticyclonic (Cyclonic and Westerlies) types tend to be underestimated (overestimated) during winter in some models. These biases have also been observed in previous evaluations concerning the previous generation of CMIP and when using an extended set of CCs. Stryhal and Huth (2019a) found that meridional circulation tends to be underestimated as models prioritize zonal advection of air masses coming from the ocean onto the continent. Furthermore, we can observe the distinction in the seasonality of some of the circulation patterns that are strongly driven by tighter meridional temperature and pressure gradients during DJF, influencing, for example, the higher (lower) frequencies of the W (LF) days, whereas JJA depicts the opposite effect. The remaining CTs' relative frequencies (Figure S3, Supporting Information) showed a better agreement for the low-frequency types between the reanalyses and GCMs. However, summer remains the best outcome.

The resulting evaluation of the SI, employed to measure the datasets' ability to capture the climatological relative frequencies of the synoptic circulations, is shown in Figure 6a. The best agreement results from the ERA-20C reanalysis during both seasons, although this dataset only assimilates surface pressure and marine wind data. However, it is likely that the resulting highest skill, compared to ERA5, is due to both datasets having closer configurations as the same centre develops them. The NOAA-20CRv3 reanalysis only outperforms the rest of the GCMs during winter. Interestingly, the skill of the JJA climatological relative frequencies in 20CRv3 appears to be similar to the captured by some of the models. The best SI scores among the GCMs arise in the UKESM, HadGEM and ECEarth GCMs that can better capture winter and summer seasons' climate state of the synoptic patterns. The remaining models generally show better performance in either one season or the other. Furthermore, IPSL has the most significant difference between the two seasons, with winter resulting in the lowest score while summer outperforms all other models. Nevertheless, none of the examined GCMs show SI values larger than 1, which indicates that none displays a lower simulation performance than the climatological ERA5 reproduced CTs.

The evaluation of the stdSI, used to measure the skill of the reanalyses and models to capture the interannual variability of the CTs adequately, is shown in Figure 6b. As before, results agree with the highest quality from the reanalyses, and ERA-20C having a slightly better skill than NOAA-20CRv3. The HadGEM climate model stands out; it better captures the year-to-year circulation variability during the reference period of 1981–2010. Yet, differences with the other models remain minimal, with

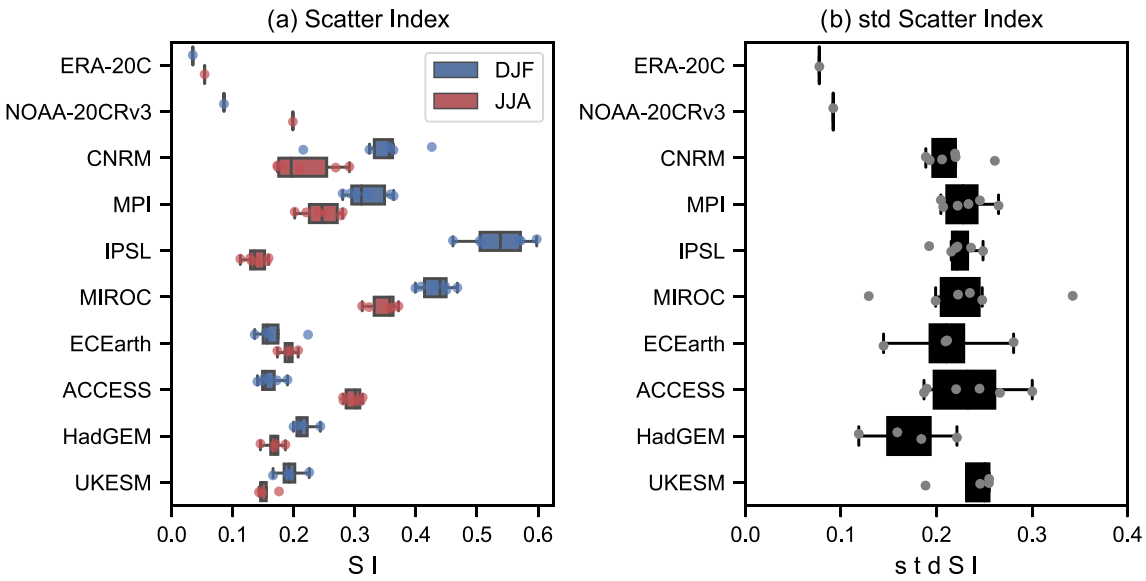

FIGURE 6 (a) Scatter index, based on climatological relative frequencies of winter (DJF) and summer (JJA). (b) Scatter index of the standard deviations, based on 30 years of yearly relative frequencies. Both analyses use the 1981–2010 period. Boxplots are based on the skills computed from all members of the GCMs where each realization skill is displayed as dots [Colour figure can be viewed at wileyonlinelibrary.com]

most of the members having skills between 0.2 and 0.25 and barely reaching values above 0.3. Similar results were found in evaluations carried out in previous versions of CMIP over the northeast Atlantic domain (Perez *et al*., 2014) and in Europe, where GCMs generally perform better (worse) during summer and autumn (spring and winter) seasons due to the low variability of the pressure input fields (Otero *et al*., 2018).

Added information results from the detected overall good ability of the datasets to capture their temporal (seasonal) characteristics based on their relative frequencies. The observed capability of the JK classification to reproduce these predefined synoptic features does not come as a surprise and instead serves as a confirmation that the CC, when applied correctly to the models, can reproduce the synoptic features correctly. This is true especially in our application, given that all the data has been brought to a joint resolution making it easier to compare between different data sources. However, even if most of the GCMs seen here demonstrate to reproduce the CTs' seasonal features, some substantial differences remain from one CT to another and among models. Intriguingly, it seems as if the model with the coarser original resolution (IPSL-CM6A-LR) relates to the worst observed performance during DJF. However, this cannot explain the results in some of the other GCMs. Further investigation on this is required using a multimodel approach to diminish the uncertainties coming from individual models, as previously suggested by Otero *et al*. (2018).

4.2 | Evaluation of past and future trends

Our investigation of frequency changes of the CTs is divided into past (1900–2010) and future (2015–2100). Trends are portrayed as relative trend magnitudes to facilitate comparability among the different data sources; only those with significance above 90% are shown (Figure 7a–d). GCM-based trend evaluation was performed using the ensemble mean seasonal relative frequencies. In addition to the historical experiment from CMIP6, we also include the ERA-20C and NOAA-20CRv3 reanalyses to compare their past trends against results from the global models.

The first noticeable difference between computed past (1900–2010) and future (2015–2100) trends is that most emerging changes do not appear during the last century but become more apparent under the chosen high-emission scenario. Nevertheless, it is possible to see that during past summers, most models show an increasing frequency of Low Flow days, whereas NOAA reanalyses indicate a decreasing trend of this CT. This contradictory finding has been addressed by Delaygue *et al*. (2019), who conclude that such behaviour relates to lacking homogeneity in observed data before the 1900s. However, the level of disagreement and the lack of consistent emerging trends between reanalyses and global models to evaluate the past does not allow drawing any feasible conclusion about possible changes in seasonal circulation frequencies in the 1900–2010 period. In contrast, the future shows a higher number of significant trends and better agreement among the models. DJF partially reveals a decreasing trend in cyclonic, E and SE types and increasing westerly dominant circulations. This corresponds to recent findings, suggesting an increase in frequency and persistence of the positive phase of the North Atlantic Oscillation, evaluated in both the CMIP5 and CMIP6 multiple scenarios (Fabiano *et al*., 2021).

On the other hand, JJA exhibits the highest number of trends. The increasing frequency in the LF types continues, as observed earlier in some models during the past period. Such projected increase has previously been documented (Otero *et al*., 2018) during summer and autumn seasons, suggesting that "weak flow" types are expected to increase in occurrence, extending from the Mediterranean towards continental Europe. We also find a divided behaviour, where most westerly-related circulations suggest decreasing frequencies while the contrary is observed in easterly-dominated types. This is likely related to projected decreasing values in the climatological SLP for JJA across most southern Europe, and primarily the Mediterranean (IPCC, 2007; Giorgi and Lionello, 2008) which has also been observed in most of the GCMs studied here (Figure S4). This could be linked to the projected poleward expansion of the Hadley cell in both CMIP5 and CMIP6 experiments (Grise and Davis, 2020).

Interestingly, a previous exploration employing winter (October–March) and summer (April–September) half years revealed the same trend signs between the different datasets but with distinctively weaker magnitudes. A slightly smaller number of statistically significant detected trends were also observed in some of the GCMs. This is likely caused due to the trends not always being consistent between DJF/JJA and the transitions seasons (MAM and SON). Further understanding would benefit by exploring whether some of these detected changes during the winter and summer meteorological seasons will extend their influence on the spring and autumn periods given the occurrence and persistency changes and their direct implications for European surface temperatures.

Recent studies argue that there is a lack of CT changes over Central Europe, given that most changes remain small and constrained within their internal

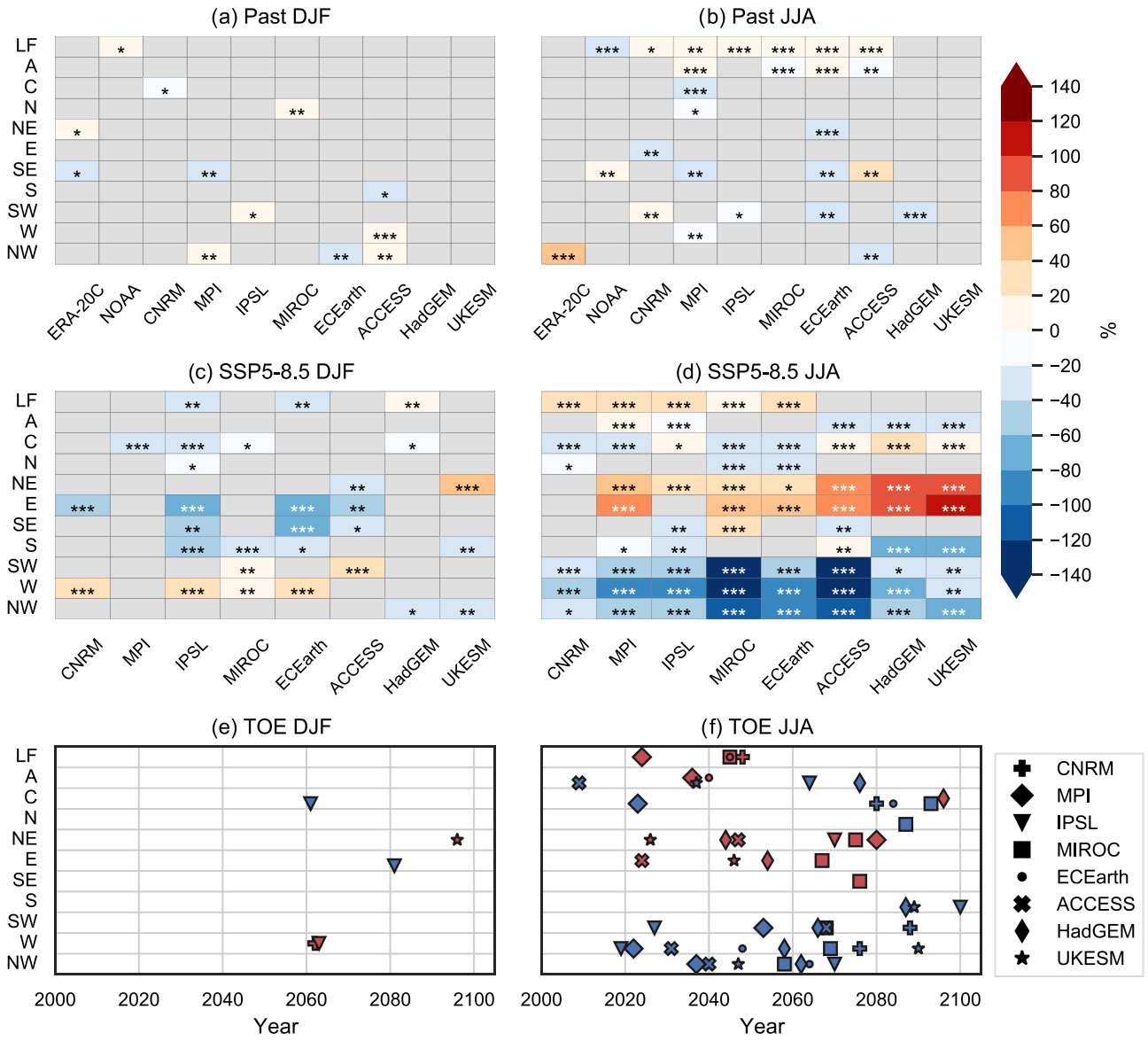

FIGURE 7 (a–d) Relative trend magnitudes, based on the Theil–Sen estimator and (e, f) TOE for DJF and JJA. Trends in the GCMs were computed along the mean of ensemble's seasonal relative frequencies. Past trends use the 1900–2010 period (a, b), while future trends are based on SSP5-8.5, covering the 2015–2100 timespan (c, d). Only significant trends are shown, based on the 90(*), 95(**) and 99(***) percentile confidence intervals, calculated with the Mann–Kendall trend test. Time of Emergence (TOE) in years corresponding to each GCM (e, f) shows only those significant emerging signals corresponding to the trends in the SSP5-8.5 scenario. Red (blue) symbols represent the positive (negative) signals surpassing the 90th(10th) percentile [Colour figure can be viewed at wileyonlinelibrary.com]

variability (Huguenin *et al.*, 2020). To investigate whether these changes in seasonal frequencies are susceptible to emerge from past variability observed in the early 20th century, we investigate their time of emergence. Mean seasonal relative frequencies are used, computed along the model's members, to derive TOE and the thresholds based on the 90th and 10th percentiles corresponding to the 1900–1950 period. TOEs in Figure 7e,f summarize these results as the corresponding emerging year of each model. Positive and negative signals are depicted as red and blue symbols, respectively. We notice that most emerging signals are detected during the summer season. Few winter circulations emerge from the "noise" of past climate under our current methodology, with most emerging trends related to those falling below the 10th percentile. This can be attributed to inherent higher variability between the circulation patterns observed during winter years, making it more challenging to detect consistently emerging signals.

As observed before in the evaluation of the future summer trends, some of these projected changes in circulation frequencies are more likely to emerge from past

variability towards the mid-21st century under the SSP5-8.5 scenario. In some cases, the detected signals vary significantly from one model to another, primarily observable in the Low Flow circulations. Some of these signals have already emerged in the ACCESS and IPSL models compared to the early 20th-century variability. Other emerging signals like those dominated by a westerly component appear more consistently ±20 years around 2050. However, the uncertainty in the years of emerging trends for most of the CTs remains high. It is strongly affected by the preferred thresholds or when they are evaluated individually along every model member. Furthermore, the current selection of a limited number of GCMs and the use of only one CC proves a limitation as it has been previously pointed out that the use of different CCs might sometimes lead to diverging conclusions as well as when employing a limited number of few GCMs (Cahynová and Huth, 2016; Kučerová *et al*., 2017; Stryhal and Huth, 2017; 2019b).

5 | SUMMARY AND CONCLUSIONS

We adapted the JC automated classification (Jenkinson and Collison, 1977), focusing on Central Europe, to determine large-scale daily circulation patterns characterized by their SLP features. Daily patterns were computed from three sets of reanalyses and eight global models from CMIP6. Data were analysed during the winter and summer seasons, with the best temporal agreement resulting from the derived circulation patterns from the reanalyses. However, some models have difficulties reproducing two of the main seasonal circulation frequencies during the winter, likely due to our chosen methodology when merging some CTs.

We can show that this classification works well in capturing single synoptic circulation patterns over Central Europe. Composites of SLP and their anomalies deliver consistent results. They only differ in the seasonality of the meridional pressure gradients, as expected. JC classification reproduces the effect of circulation patterns on daily temperature anomalies over Europe. Further work is needed to evaluate the capability of GCMs to capture these effects.

The obtained CTs, based on global models and reanalyses, were generally able to reproduce key climatological features of the synoptic types for the 1981–2010 period. Most models clearly show different skills depending on the analysed season. Summer appears to result in the highest skills on most of the ensemble members between the models. The ability to capture the interannual variability outperforms in the ERA-20C and NOAA-20CRv3 reanalyses. While the GCMs generally portray the same mean ability, only the HadGEM model slightly outpaces the others. Despite recently reported improvement in CMIP6 models' ability to reproduce the synoptic features over Europe when compared to the previous CMIP5 (Fernandez-Granja *et al*., 2021), some models analysed here, for example, IPSL and MIROC, still, show biases when capturing frequencies of the major CTs.

The ERA5 maps showing the composites of mean SLP fields and their anomalies from the derived synoptic circulation types demonstrate that the classification correctly discerns the spatial configuration of the large-scale atmospheric circulations. Furthermore, the T2M anomalies associated with each CT show the strong link between the influence of circulation patterns on temperature advection over Europe. This becomes more noticeable for some low-frequency types, such as the Easterly and Westerly types, that are usually associated with opposite temperature effects depending on the analysed period.

Evaluating past and future trends in CTs' seasonal frequencies shows that most tendencies emerge during JJA in the SSP5-8.5 scenario. The highest agreement relates to a likely frequency increase of days classified as "weak flow" (LF type) in eastern and northeastern types and a decrease in days characterized by all the westerly components. The projected increase in LF-days dominated by weak airflow and stationary air masses agrees with findings on an increment in future episodes of air pollution (Horton *et al*., 2012). Our results also suggest that towards the mid-21st century, these changes might emerge from past (1900–1950) variability, assuming a high-emission scenario. However, high uncertainty remains in the detected times of emergence of these signals as they can distinctly vary from one model to another. For example, in anticyclonic and westerly days, certain models suggest that some changes have already emerged during the past decade. They agree with other investigated TOEs based on temperatures over Europe, implying that temperature changes have already emerged around the start of the 21st century (Lehner *et al*., 2017). However, future European temperature changes are found not to be related to changes in CT frequency. It is somewhat expected that global warming would also affect characteristics of the synoptic circulation types (Otero *et al*., 2018). Therefore, additional assessment on understanding the drivers behind these signals remains necessary to determine the potential effects of such changes on the future European climate.

ACKNOWLEDGEMENTS

We thankfully acknowledge funding through the EU International Training Network (ITN) Climate Advanced Forecasting of sub-seasonal Extremes (CAFE). The

project is supported by the European Union's Horizon 2020 research and innovation programme under the Marie Skłodowska-Curie Grant Agreement No. 813844. We would also like to thank Paul James and Stephanie Hänsel from Deutscher Wetterdienst, Philip Jones from the University of East Anglia and Gilles Delaygue from the University Grenoble-Alpes for their availability and fruitful discussions during the development of this work.

AUTHOR CONTRIBUTIONS

Pedro Herrera-Lormendez: Conceptualization; data curation; formal analysis; investigation; methodology; visualization; writing – original draft. **Nikolaos Mastrantonas:** Methodology; validation; visualization; writing – review and editing. **Herve Douville:** Methodology; supervision; validation; writing – review and editing. **Andreas Hoy:** Resources; validation; writing – review and editing. **Jörg Matschullat:** Conceptualization; supervision; writing – review and editing.

ORCID

Pedro Herrera-Lormendez https://orcid.org/0000-0003-0982-0032
Nikolaos Mastrantonas https://orcid.org/0000-0002-2430-3634
Hervé Douville https://orcid.org/0000-0002-6074-6467
Andreas Hoy https://orcid.org/0000-0003-3733-6483
Jörg Matschullat https://orcid.org/0000-0003-0549-7354

REFERENCES

EC-Earth. (2019) *EC-Earth-Consortium EC-Earth3 model output prepared for CMIP6 CMIP*. Version 20200701. Earth System Grid Federation. https://doi.org/10.22033/ESGF/CMIP6.181.

Barnes, E.A., Dunn-Sigouin, E., Masato, G. and Woollings, T. (2014) Exploring recent trends in Northern Hemisphere blocking. *Geophysical Research Letters*, 41(2), 638–644. https://doi.org/10.1002/2013GL058745.

Baur, F., Hess, P. and Nagel, H. (1944) *Kalendar der Groswetterlagen Europas 1881—1939*. Bad Homburg.

Beck, C., Jacobeit, J. and Jones, P.D. (2007) Frequency and within-type variations of large-scale circulation types and their effects on low-frequency climate variability in Central Europe since 1780. *International Journal of Climatology*, 27(4), 473–491. https://doi.org/10.1002/joc.1410.

Beck, C. and Philipp, A. (2010) Evaluation and comparison of circulation type classifications for the European domain. *Physics and Chemistry of the Earth*, 35(9–12), 374–387. https://doi.org/10.1016/j.pce.2010.01.001.

Belleflamme, A., Fettweis, X. and Erpicum, M. (2015) Do global warming-induced circulation pattern changes affect temperature and precipitation over Europe during summer? *International Journal of Climatology*, 35(7), 1484–1499. https://doi.org/10.1002/joc.4070.

Boucher, O., Denvil, S., Levavasseur, G., Cozic, A., Caubel, A., Foujols, M. A., Meurdesoif, Y., Cadule, P., Devilliers, M., Ghattas, J., Lebas, N., Lurton, T., Mellul, L., Musat, I., Mignot, J. and Cheruy, F. (2018) *IPSL IPSL-CM6A-LR model output prepared for CMIP6 CMIP*. Version 20200701. Earth System Grid Federation. https://doi.org/10.22033/ESGF/CMIP6.1534.

Cahynová, M. and Huth, R. (2016) Atmospheric circulation influence on climatic trends in Europe: an analysis of circulation type classifications from the COST733 catalogue. *International Journal of Climatology*, 36(7), 2743–2760. https://doi.org/10.1002/joc.4003.

Cattiaux, J., Peings, Y., Saint-Martin, D., Trou-Kechout, N. and Vavrus, S.J. (2016) Sinuosity of midlatitude atmospheric flow in a warming world. *Geophysical Research Letters*, 43(15), 8259–8268. https://doi.org/10.1002/2016GL070309.

de Vries, H., Woollings, T., Anstey, J., Haarsma, R.J. and Hazeleger, W. (2013) Atmospheric blocking and its relation to jet changes in a future climate. *Climate Dynamics*, 41(9-10), 2643–2654. https://doi.org/10.1007/s00382-013-1699-7

Delaygue, G., Brönnimann, S., Jones, P.D., Blanchet, J. and Schwander, M. (2019) Reconstruction of Lamb weather type series back to the eighteenth century. *Climate Dynamics*, 52(9-10), 6131–6148. https://doi.org/10.1007/s00382-018-4506-7

El Kenawy, A.M., McCabe, M.F., Stenchikov, G.L. and Raj, J. (2014) Multi-decadal classification of synoptic weather types, observed trends and links to rainfall characteristics over Saudi Arabia. *Frontiers in Environmental Science*, 2. https://doi.org/10.3389/fenvs.2014.00037

Eyring, V., Bony, S., Meehl, G.A., Senior, C.A., Stevens, B., Stouffer, R.J. and Taylor, K.E. (2016) Overview of the Coupled Model Intercomparison Project Phase 6 (CMIP6) experimental design and organization. *Geoscientific Model Development*, 9(5), 1937–1958. https://doi.org/10.5194/gmd-9-1937-2016

Fabiano, F., Meccia, V.L., Davini, P., Ghinassi, P. and Corti, S. (2021) A regime view of future atmospheric circulation changes in northern mid-latitudes. *Weather and Climate Dynamics*, 2(1), 163–180. https://doi.org/10.5194/wcd-2-163-2021.

Fernandez-Granja, J.A., Casanueva, A., Bedia, J. and Fernandez, J. (2021) Improved atmospheric circulation over Europe by the new generation of CMIP6 earth system models. *Climate Dynamics*, 56, 1–14. https://doi.org/10.1007/s00382-021-05652-9.

Giorgi, F. and Lionello, P. (2008) Climate change projections for the Mediterranean region. *Global and Planetary Change*, 63(2–3), 90–104. https://doi.org/10.1016/j.gloplacha.2007.09.005.

Goodess, C.M. and Jones, P.D. (2002) Links between circulation and changes in the characteristics of Iberian rainfall. *International Journal of Climatology*, 22(13), 1593–1615. https://doi.org/10.1002/joc.810.

Grise, K.M. and Davis, S.M. (2020) Hadley cell expansion in CMIP6 models. *Atmospheric Chemistry and Physics*, 20(9), 5249–5268. https://doi.org/10.5194/acp-20-5249-2020.

Hannaford, J., Mastrantonas, N., Vesuviano, G. and Turner, S. (2021) An updated national-scale assessment of trends in UK peak river flow data: how robust are observed increases in flooding? *Hydrology Research*, 52, 699–718. https://doi.org/10.2166/nh.2021.156.

Harrigan, S., Hannaford, J., Muchan, K. and Marsh, T.J. (2018) Designation and trend analysis of the updated UK Benchmark

Network of river flow stations: the UKBN2 dataset. *Hydrology Research*, 49(2), 552–567. https://doi.org/10.2166/nh.2017.058

Hersbach, H., Bell, B., Berrisford, P., Hirahara, S., Horányi, A., Muñoz-Sabater, J., Nicolas, J., Peubey, C., Radu, R., Schepers, D., Simmons, A., Soci, C., Abdalla, S., Abellan, X., Balsamo, G., Bechtold, P., Biavati, G., Bidlot, J., Bonavita, M., Chiara, G., Dahlgren, P., Dee, D., Diamantakis, M., Dragani, R., Flemming, J., Forbes, R., Fuentes, M., Geer, A., Haimberger, L., Healy, S., Hogan, R.J., Hólm, E., Janisková, M., Keeley, S., Laloyaux, P., Lopez, P., Lupu, C., Radnoti, G., Rosnay, P., Rozum, I., Vamborg, F., Villaume, S. and Thépaut, J.N. (2020) The ERA5 global reanalysis. *Quarterly Journal of the Royal Meteorological Society*, 146(730), 1999–2049. https://doi.org/10.1002/qj.3803.

Hess, P. and Breszowsky, H. (1952) Katalog der Großwetterlagen Europas. *Ber. Dt. Wetterd. in der USZone*, 33.

Horton, D.E., Harshvardhan and Diffenbaugh, N.S. (2012) Response of air stagnation frequency to anthropogenically enhanced radiative forcing. *Environmental Research Letters*, 7(4), 44034–44043. https://doi.org/10.1088/1748-9326/7/4/044034.

Hoy, A., Schucknecht, A., Sepp, M. and Matschullat, J. (2014) Large-scale synoptic types and their impact on European precipitation. *Theoretical and Applied Climatology*, 116(1–2), 19–35. https://doi.org/10.1007/s00704-013-0897-x.

Hoy, A., Sepp, M. and Matschullat, J. (2013a) Atmospheric circulation variability in Europe and northern Asia (1901 to 2010). *Theoretical and Applied Climatology*, 113(1–2), 105–126. https://doi.org/10.1007/s00704-012-0770-3.

Hoy, A., Sepp, M. and Matschullat, J. (2013b) Large-scale atmospheric circulation forms and their impact on air temperature in Europe and northern Asia. *Theoretical and Applied Climatology*, 113(3–4), 643–658. https://doi.org/10.1007/s00704-012-0813-9.

Huguenin, M.F., Fischer, E.M., Kotlarski, S., Scherrer, S.C., Schwierz, C. and Knutti, R. (2020) Lack of change in the projected frequency and persistence of atmospheric circulation types over Central Europe. *Geophysical Research Letters*, 47(9). https://doi.org/10.1029/2019GL086132.

Hussain, M. and Mahmud, I. (2019) pyMannKendall: a python package for non parametric Mann Kendall family of trend tests. *Journal of Open Source Software*, 4(39), 1556https://doi.org/10.21105/joss.01556.

Huth, R., Beck, C., Philipp, A., Demuzere, M., Ustrnul, Z., Cahynová, M., Kyselý, J. and Tveito, O.E. (2008) Classifications of atmospheric circulation patterns: recent advances and applications. *Annals of the New York Academy of Sciences*, 1146, 105–152. https://doi.org/10.1196/annals.1446.019.

Jacobeit, J., Homann, M., Philipp, A. and Beck, C. (2017) Atmospheric circulation types and extreme areal precipitation in southern Central Europe. *Advances in Science and Research*, 14, 71–75. https://doi.org/10.5194/asr-14-71-2017.

Jacobeit, J., Wanner, H., Luterbacher, J., Beck, C., Philipp, A. and Sturm, K. (2003) Atmospheric circulation variability in the North-Atlantic-European area since the mid-seventeenth century. *Climate Dynamics*, 20(4), 341–352. https://doi.org/10.1007/s00382-002-0278-0.

Jenkinson, A.F. and Collison, F.P. (1977) *An initial climatology of gales over the North Sea*. Bracknell: Meteorological Office. Synoptic Climatology Branch Memorandum No. 62.

Jones, P.D., Harpham, C. and Briffa, K.R. (2013) Lamb weather types derived from reanalysis products. *International Journal of Climatology*, 33(5), 1129–1139. https://doi.org/10.1002/joc.3498.

Jones, P.D., Harpham, C. and Lister, D. (2016) Long-term trends in gale days and storminess for The Falkland Islands. *International Journal of Climatology*, 36(3), 1413–1427. https://doi.org/10.1002/joc.4434.

Jones, P.D., Hulme, M. and Briffa, K.R. (1993) A comparison of Lamb circulation types with an objective classification scheme. *International Journal of Climatology*, 13(6), 655–663. https://doi.org/10.1002/joc.3370130606.

Jones, P.D., Osborn, T.J., Harpham, C. and Briffa, K.R. (2014) The development of Lamb weather types: from subjective analysis of weather charts to objective approaches using reanalyses. *Weather*, 69(5), 128–132. https://doi.org/10.1002/wea.2255.

Khairul, I.M., Mastrantonas, N., Rasmy, M., Koike, T. and Takeuchi, K. (2018) Inter-comparison of gauge-corrected global satellite rainfall estimates and their applicability for effective water resource management in a transboundary river basin: the case of the Meghna River basin. *Remote Sensing*, 10(6), 828https://doi.org/10.3390/rs10060828.

Kučerová, M., Beck, C., Philipp, A. and Huth, R. (2017) Trends in frequency and persistence of atmospheric circulation types over Europe derived from a multitude of classifications. *International Journal of Climatology*, 37(5), 2502–2521. https://doi.org/10.1002/joc.4861.

Lai, I.-C. (2010) *The relationship between tropospheric ozone and atmospheric circulation in Taiwan*. PhD Thesis, University of East Anglia.

Lamb, H.H. (1972) *British Isles Weather Types and a Register of Daily Sequence of Circulation Patterns*, 116, 1861–1971. H.M. Stationery Office. *Geophysical Memoir*.

Lehner, F., Deser, C. and Terray, L. (2017) Toward a new estimate of "time of emergence" of anthropogenic warming: insights from dynamical adjustment and a large initial-condition model ensemble. *Journal of Climate*, 30(19), 7739–7756. https://doi.org/10.1175/JCLI-D-16-0792.1.

Linderson, M.L. (2001) Objective classification of atmospheric circulation over Southern Scandinavia. *International Journal of Climatology*, 21(2), 155–169. https://doi.org/10.1002/joc.604.

Lorenzo, M.N., Ramos, A.M., Taboada, J.J. and Gimeno, L. (2011) Changes in present and future circulation types frequency in northwest iberian peninsula. *PLoS ONE*, 6(1), e16201. https://doi.org/10.1371/journal.pone.0016201

Maraun, D. (2013) When will trends in European mean and heavy daily precipitation emerge?. *Environmental Research Letters*, 8, 014004. https://doi.org/10.1088/1748-9326/8/1/014004

Mastrantonas, N., Bhattacharya, B., Shibuo, Y., Rasmy, M., Espinoza-Dávalos, G. and Solomatine, D. (2019) Evaluating the benefits of merging near-real-time satellite precipitation products: a case study in the Kinu basin region, Japan. *Journal of Hydrometeorology*, 20(6), 1213–1233. https://doi.org/10.1175/JHM-D-18-0190.1.

Mastrantonas, N., Herrera-Lormendez, P., Magnusson, L., Pappenberger, F. and Matschullat, J. (2021) Extreme precipitation events in the Mediterranean: spatiotemporal characteristics and connection to large-scale atmospheric flow patterns. *International Journal of Climatology*, 41(4), 2710–2728. https://doi.org/10.1002/joc.6985.

Meehl, G.A. and Tebaldi, C. (2004) More Intense, More Frequent, and Longer Lasting Heat Waves in the 21st Century. *Science*, 305(5686), 994–997. https://doi.org/10.1126/science.1098704

IPCC (2007). In: Solomon, S., Qin, D., Manning, M., Chen, Z., Marquis, M., Averyt, K.B., Tignor, M. & Miller, H.L., (eds), *Climate Change 2007: The Physical Science Basis. Contribution of Working Group I to the Fourth Assessment Report of the Intergovernmental Panel on Climate Change*, Vol. 54. Cambridge, UK and New York, NY: Cambridge University Press, pp. 747–845.

O'Neill, B.C., Kriegler, E., Ebi, K.L., Kemp-Benedict, E., Riahi, K., Rothman, D.S., van Ruijven, B.J., van Vuuren, D.P., Birkmann, J., Kok, K., Levy, M. and Solecki, W. (2015) The roads ahead: narratives for shared socioeconomic pathways describing world futures in the 21st century. *Global Environmental Change*, 42, 169–180. https://doi.org/10.1016/j.gloenvcha.2015.01.004.

Otero, N., Sillmann, J. and Butler, T. (2018) Assessment of an extended version of the Jenkinson–Collison classification on CMIP5 models over Europe. *Climate Dynamics*, 50(5–6), 1559–1579. https://doi.org/10.1007/s00382-017-3705-y.

Parker, W.S. (2016) Reanalyses and Observations: What's the Difference?. *Bulletin of the American Meteorological Society*, 97(9), 1565–1572. https://doi.org/10.1175/bams-d-14-00226.1

Perez, J., Menendez, M., Mendez, F.J. and Losada, I.J. (2014) Evaluating the performance of CMIP3 and CMIP5 global climate models over the north-east Atlantic region. *Climate Dynamics*, 43(9–10), 2663–2680. https://doi.org/10.1007/s00382-014-2078-8.

Poli, P., Hersbach, H., Dee, D.P., Berrisford, P., Simmons, A.J., Vitart, F., Laloyaux, P., Tan, D.G.H., Peubey, C., Thépaut, J.N., Trémolet, Y., Hólm, E.V., Bonavita, M., Isaksen, L. and Fisher, M. (2016) ERA-20C: an atmospheric reanalysis of the twentieth century. *Journal of Climate*, 29(11), 4083–4097. https://doi.org/10.1175/JCLI-D-15-0556.1.

Räisänen, J. (2019) Effect of atmospheric circulation on recent temperature changes in Finland. *Climate Dynamics*, 53(9–10), 5675–5687. https://doi.org/10.1007/s00382-019-04890-2.

Riahi, K., van Vuuren, D.P., Kriegler, E., Edmonds, J., O'Neill, B.C., Fujimori, S., Bauer, N., Calvin, K., Dellink, R., Fricko, O., Lutz, W., Popp, A., Cuaresma, J.C., Kc, S., Leimbach, M., Jiang, L., Kram, T., Rao, S., Emmerling, J., Ebi, K., Hasegawa, T., Havlik, P., Humpenöder, F., da Silva, L.A., Smith, S., Stehfest, E., Bosetti, V., Eom, J., Gernaat, D., Masui, T., Rogelj, J., Strefler, J., Drouet, L., Krey, V., Luderer, G., Harmsen, M., Takahashi, K., Baumstark, L., Doelman, J.C., Kainuma, M., Klimont, Z., Marangoni, G., Lotze-Campen, H., Obersteiner, M., Tabeau, A. and Tavoni, M. (2017) The shared socioeconomic pathways and their energy, land use, and greenhouse gas emissions implications: an overview. *Global Environmental Change*, 42, 153–168. https://doi.org/10.1016/j.gloenvcha.2016.05.009.

Richardson, D., Neal, R., Dankers, R., Mylne, K., Cowling, R., Clements, H. and Millard, J. (2020) Linking weather patterns to regional extreme precipitation for highlighting potential flood events in medium- to long-range forecasts. *Meteorological Applications*, 27(4). https://doi.org/10.1002/met.1931.

Ridley, J., Menary, M., Kuhlbrodt, T., Andrews, M. and Andrews, T. (2018) *MOHC HadGEM3-GC31-LL model output prepared for CMIP6 CMIP*. Version 20200701. Earth System Grid Federation. https://doi.org/10.22033/ESGF/CMIP6.419.

Russo, S., Sillmann, J. and Fischer, E.M. (2015) Top ten European heatwaves since 1950 and their occurrence in the coming decades. *Environmental Research Letters*, 10(12), 124003. https://doi.org/10.1088/1748-9326/10/12/124003.

Sarricolea Espinoza, P., Meseguer-Ruiz, Ó. and Martín Vide, J. (2014) Variabilidad y tendencias climáticas en Chile central en el período 1950-2010 mediante la determinación de los tipos sinópticos de Jenkinson y Collison. *Boletín de la Asociación de Geógrafos Españoles*, 64, 227–247. https://doi.org/10.21138/bage.1688.

Seneviratne, S.I., Nicholls, N, Easterling, D., Goodess, C.M., Kanae, S., Kossin, J., Luo, Y., Marengo, J., Mc Innes, K., Rahimi, M., Reichstein, M., Sorteberg, A., Vera, Z., Zhang, X., Rusticucci, N., Semenov, V., Alexander, L.V., Allen, S., Benito, G., Cavazos, T., Clague, J., Conway, D., Della-Marta, P. M., Gerber, M., Gong, S., Goswami, B.N., Hemer, M., Huggel, C., Van den Hurk, B., Kharin, V.V., Kitoh, A., Klein Tank, A.M.G., Li, G., Mason, S., Mc Guire, W., Van Oldenborgh, G.J., Orlowsky, B., Smith, S., Thiaw, W., Velegrakis, A., Yiou, P., Zhang, T., Zhou, T. and Zwiers, F.W. (2012) Changes in climate extremes and their impacts on the natural physical environment. *Managing the risks of extreme events and disasters to advance climate change adaptation: Special report of the intergovernmental panel on climate change*. Cambridge University Press. 109–230.

Schoetter, R., Cattiaux, J. and Douville, H. (2015) Changes of western European heat wave characteristics projected by the CMIP5 ensemble. *Climate Dynamics*, 45(5–6), 1601–1616. https://doi.org/10.1007/s00382-014-2434-8.

Schüepp, M. (1979) *Klimatologie der Schweiz. Band III: Witterungsklimatologie*. Zurich: Schweizerische Meteorologische Anstalt.

Schwalm, C.R., Glendon, S. and Duffy, P.B. (2020) RCP8.5 tracks cumulative CO_2 emissions. *Proceedings of the National Academy of Sciences of the United States of America*, 117(33), 19656–19657. https://doi.org/10.1073/PNAS.2007117117.

Schwander, M., Brönnimann, S., Delaygue, G., Rohrer, M., Auchmann, R. and Brugnara, Y. (2017) Reconstruction of Central European daily weather types back to 1763. *International Journal of Climatology*, 37, 30–44. https://doi.org/10.1002/joc.4974.

Shepherd, T.G. (2014) Atmospheric circulation as a source of uncertainty in climate change projections. *Nature Geoscience*, 7(10), 703–708. https://doi.org/10.1038/ngeo2253

Slivinski, L.C., Compo, G.P., Whitaker, J.S., Sardeshmukh, P.D., Giese, B.S., McColl, C., Allan, R., Yin, X., Vose, R., Titchner, H., Kennedy, J., Spencer, L.J., Ashcroft, L., Brönnimann, S., Brunet, M., Camuffo, D., Cornes, R., Cram, T. A., Crouthamel, R., Domínguez-Castro, F., Freeman, J.E., Gergis, J., Hawkins, E., Jones, P.D., Jourdain, S., Kaplan, A., Kubota, H., Blancq, F.L., Lee, T.C., Lorrey, A., Luterbacher, J., Maugeri, M., Mock, C.J., Moore, G.W.K., Przybylak, R., Pudmenzky, C., Reason, C., Slonosky, V.C., Smith, C.A., Tinz, B., Trewin, B., Valente, M.A., Wang, X.L., Wilkinson, C., Wood, K. and Wyszyński, P. (2019) Towards a more reliable historical reanalysis: improvements for version 3 of the twentieth century reanalysis system. *Quarterly Journal of the Royal*

Meteorological Society, 145(724), 2876–2908. https://doi.org/10.1002/qj.3598.

Spellman, G. (2017) An assessment of the Jenkinson and Collison synoptic classification to a continental mid-latitude location. *Theoretical and Applied Climatology*, 128(3–4), 731–744. https://doi.org/10.1007/s00704-015-1711-8.

Stryhal, J. and Huth, R. (2017) Classifications of winter Euro-Atlantic circulation patterns: an intercomparison of five atmospheric reanalyses. *Journal of Climate*, 30(19), 7847–7861. https://doi.org/10.1175/JCLI-D-17-0059.1.

Stryhal, J. and Huth, R. (2019a) Classifications of winter atmospheric circulation patterns: validation of CMIP5 GCMs over Europe and the North Atlantic. *Climate Dynamics*, 52(5–6), 3575–3598. https://doi.org/10.1007/s00382-018-4344-7.

Stryhal, J. and Huth, R. (2019b) Trends in winter circulation over the British Isles and Central Europe in twenty-first century projections by 25 CMIP5 GCMs. *Climate Dynamics*, 52(1–2), 1063–1075. https://doi.org/10.1007/s00382-018-4178-3.

Tang, Y., Rumbold, S., Ellis, R., Kelley, D., Mulcahy, J., Sellar, A., Walton, J. and Jones, C. (2019) *MOHC UKESM1.0-LL model output prepared for CMIP6 CMIP*. Version 20200701. Earth System Grid Federation. https://doi.org/10.22033/ESGF/CMIP6.6113.

Tatebe, H. and Watanabe, M. (2018) *MIROC MIROC6 model output prepared for CMIP6 CMIP*. Version 20200701. Earth System Grid Federation. https://doi.org/10.22033/ESGF/CMIP6.881.

Vallorani, R., Bartolini, G., Betti, G., Crisci, A., Gozzini, B., Grifoni, D., Iannuccilli, M., Messeri, A., Messeri, G., Morabito, M. and Maracchi, G. (2018) Circulation type classifications for temperature and precipitation stratification in Italy. *International Journal of Climatology*, 38(2), 915–931. https://doi.org/10.1002/joc.5219.

Voldoire, A. (2018) *CNRM-CERFACS CNRM-CM6-1 model output prepared for CMIP6 CMIP*. Version 20200701. Earth System Grid Federation. https://doi.org/10.22033/ESGF/CMIP6.1375.

Wieners, K.-H., Giorgetta, M., Jungclaus, J., Reick, C., Esch, M., Bittner, M., Legutke, S., Schupfner, M., Wachsmann, F., Gayler, V., Haak, H., de Vrese, P., Raddatz, T., Mauritsen, T., von Storch, J. S., Behrens, J., Brovkin, V., Claussen, M., Crueger, T., Fast, I., Fiedler, S., Hagemann, S., Hohenegger, C., Jahns, T., Kloster, S., Kinne, S., Lasslop, G., Kornblueh, L., Marotzke, J., Matei, D., Meraner, K., Mikolajewicz, U., Modali, K., Müller, W., Nabel, J., Notz, D., Peters-von Gehlen, K., Pincus, R., Pohlmann, H., Pongratz, J., Rast, S., Schmidt, H., Schnur, R., Schulzweida, U., Six, K., Stevens, B., Voigt, A. and Roeckner, E. (2019) *MPI-M MPIESM1.2-LR model output prepared for CMIP6 CMIP*. Version 20200701. Earth System Grid Federation. https://doi.org/10.22033/ESGF/CMIP6.742.

Woollings, T., Barriopedro, D., Methven, J., Son, S.W., Martius, O., Harvey, B., Sillmann, J, Lupo, A.R. and Seneviratne, S. (2018) Blocking and its Response to Climate Change. *Current Climate Change Reports*, 4(3), 287–300. https://doi.org/10.1007/s40641-018-0108-z

Woollings, T., Gregory, J.M., Pinto, J.G., Reyers, M. and Brayshaw, D.J. (2012) Response of the North Atlantic storm track to climate change shaped by ocean–atmosphere coupling. *Nature Geoscience*, 5, 313–317. https://doi.org/10.1038/ngeo1438.

Yarnal, B., Comrie, A.C., Frakes, B. and Brown, D.P. (2001) Developments and prospects in synoptic climatology. *International Journal of Climatology*, 21(15), 1923–1950. https://doi.org/10.1002/joc.675.

Ziehn, T., Chamberlain, M., Lenton, A., Law, R., Bodman, R., Dix, M., Wang, Y., Dobrohotoff, P., Srbinovsky, J., Stevens, L., Vohralik, P., Mackallah, C., Sullivan, A., O'Farrell, S. and Druken, K. (2019) *CSIRO ACCESS-ESM1.5 model output prepared for CMIP6 CMIP*. Version 20200701. Earth System Grid Federation. https://doi.org/10.22033/ESGF/CMIP6.2288.

SUPPORTING INFORMATION

Additional supporting information may be found in the online version of the article at the publisher's website.

How to cite this article: Herrera-Lormendez, P., Mastrantonas, N., Douville, H., Hoy, A., & Matschullat, J. (2022). Synoptic circulation changes over Central Europe from 1900 to 2100: Reanalyses and Coupled Model Intercomparison Project phase 6. *International Journal of Climatology*, *42*(7), 4062–4077. https://doi.org/10.1002/joc.7481